Title

Nuclear organization of orexinergic neurons in the hypothalamus of a lar gibbon and a chimpanzee

Journal

The Anatomical Record, 305(6)

ISSN

1932-8486

Authors

Williams, Victoria M
Bhagwandin, Adhil
Swiegers, Jordan
et al.

Publication Date

2022-06-01

DOI

10.1002/ar.24775

Peer reviewed

HHS Public Access

Author manuscript

Anat Rec (Hoboken). Author manuscript; available in PMC 2022 June 01.

Published in final edited form as:

Anat Rec (Hoboken). 2022 June ; 305(6): 1459–1475. doi:10.1002/ar.24775.

Nuclear organization of orexinergic neurons in the hypothalamus of a lar gibbon and a chimpanzee

Victoria M. Williams[1], **Adhil Bhagwandin**[1,2], **Jordan Swiegers**[1], **Mads F. Bertelsen**[3], **Therese Hård**[4], **Thomas C. Thannickal**[5,6], **Jerome M. Siegel**[5,6], **Chet C. Sherwood**[7], **Paul R. Manger**[1]

[1]School of Anatomical Sciences, Faculty of Health Sciences, University of the Witwatersrand, Johannesburg, Republic of South Africa

[2]Division of Clinical Anatomy and Biological Anthropology, Department of Human Biology, University of Cape Town, Cape Town, South Africa

[3]Centre for Zoo and Wild Animal Health, Copenhagen Zoo, Frederiksberg, Denmark

[4]Borås Zoo, Borås, Sweden

[5]Department of Psychiatry, School of Medicine, and Brain Research Institute, University of California, Los Angeles, Los Angeles, California, USA

[6]Brain Research Institute, Neurobiology Research, Sepulveda VA Medical Center, Los Angeles, California, USA

[7]Department of Anthropology and Center for the Advanced Study of Human Paleobiology, The George Washington University, Washington, District of Columbia, USA

Abstract

Employing orexin-A immunohistochemical staining we describe the nuclear parcellation of orexinergic neurons in the hypothalami of a lar gibbon and a chimpanzee. The clustering of orexinergic neurons within the hypothalamus and the terminal networks follow the patterns generally observed in other mammals, including laboratory rodents, strepsirrhine primates and humans. The orexinergic neurons were found within three distinct clusters in the ape hypothalamus, which include the main cluster, zona incerta cluster and optic tract cluster. In addition, the orexinergic neurons of the optic tract cluster appear to extend to a more rostral

Correspondence: Paul R. Manger, School of Anatomical, Sciences, University of the Witwatersrand, 7 York Road, Parktown, 2193, Johannesburg, South Africa, paul.manger@wits.ac.za.

AUTHOR CONTRIBUTIONS

Victoria Williams: Conceptualization (equal); data curation (equal); formal analysis (equal); investigation (equal); methodology (equal); writing – original draft (equal). **Adhil Bhagwandin:** Data curation (equal); formal analysis (equal); investigation (equal); methodology (equal); writing – review and editing (equal). **Jordan Swiegers:** Formal analysis (equal); investigation (equal); methodology (equal); writing – review and editing (equal). **Mads Bertelsen:** Investigation (equal); methodology (equal); writing – review and editing (equal). **Therese Hard:** Investigation (equal); methodology (equal); writing – review and editing (equal). **Thomas Thannickal:** Formal analysis (equal); investigation (equal); methodology (equal); writing – review and editing (equal). **Jerome Siegel:** Formal analysis (equal); investigation (equal); methodology (equal); writing – review and editing (equal). **Chet C. Sherwood:** Conceptualization (equal); formal analysis (equal); funding acquisition (equal); investigation (equal); methodology (equal); supervision (equal); writing – review and editing (equal). **Paul Manger:** Conceptualization (equal); data curation (equal); formal analysis (equal); funding acquisition (equal); investigation (equal); methodology (equal); project administration (equal); supervision (equal); validation (equal); visualization (equal); writing – original draft (equal); writing – review and editing (equal).

CONFLICT OF INTEREST

The authors declare no conflicts of interest.

and medial location than observed in other species, being observed in the tuberal region in the anterior ventromedial aspect of the hypothalamus. While orexinergic terminal networks were observed throughout the brain, high density terminal networks were observed within the hypothalamus, medial and intralaminar nuclei of the dorsal thalamus, and within the serotonergic and noradrenergic regions of the midbrain and pons, which is typical for mammals. The expanded distribution of orexinergic neurons into the tuberal region of the ape hypothalamus, is a feature that needs to be investigated in other primate species, but appears to correlate with orexin gene expression in the same region of the human hypothalamus, but these neurons are not revealed with immunohistochemical staining in humans. Thus, it appears that apes have a broader distribution of orexinergic neurons compared to other primate species, but that the neurons within this extension of the optic tract cluster in humans, while expressing the orexin gene, do not produce the neuropeptide.

Keywords

ape; brain evolution; hypocretin; immunohistochemistry; orexin; primates

1 | INTRODUCTION

The orexin neuropeptides (also known as hypocretin) were originally discovered in the hypothalamus of the rat brain. Based on the relationship of the orexinergic neurons to the hypothalamic “feeding center” and their ability to stimulate food intake, orexins were coined the “regulators of appetite” (de Lecea et al., 1998). The two orexin neuropeptides are involved in many physiological and behavioral activities, such as the control of drinking behavior, neuroendocrine homeostasis, and somatic motor control (Zhang, Yu, Zhuang, Zhu, & Wang, 2013). The orexin neuropeptides also play a crucial role in the regulation of wakefulness and sleep (Chow & Cao, 2016; de Lecea & Sutcliffe, 2005). This is supported by multiple lines of evidence that associate sleep disorders, such as narcolepsy in humans, with deficiencies in the orexinergic system (e.g., Nishino, Ripley, Overeem, Lammers, & Mignot, 2000; Peyron et al., 2000; Thannickal et al., 2000). Thus, the orexinergic system appears to form the interface that balances the need to be awake, alert and active in relation to the need to obtain nutrition (Malungo, Gravett, Bhagwandin, Davimes, & Manger, 2020).

The distribution of orexinergic cell bodies and terminal networks have been described in a range of mammalian species (e.g., Davimes et al., 2017; Dell et al., 2012; Dell, Karlsson, Patzke, Spocter, Siegel, & Manger, 2016; Dell, Patzke, Spocter, Bertelsen, Siegel, & Manger, 2016; Dell, Kruger, Pettigrew, & Manger, 2013; Dell, Patzke, Spocter, Siegel, & Manger, 2016; Gravett, Bhagwandin, Fuxe, & Manger, 2011; Iqbal, Pompolo, Sakurai, & Clarke, 2001; Khorooshi & Klingenspor, 2005; Kruger, Dell, Pettigrew, & Manger, 2010; Malungo et al., 2020; Nixon & Smale, 2007; Yamamoto et al., 2006; Zhang, Sampogna, Morales, & Chase, 2002), including strepsirrhine primates (Calvey et al., 2015) and humans (Elias et al., 1998; Moore, Abrahamson, & van den Pol, 2001; Thannickal et al., 2018; Thannickal, Moore, et al., 2000; Thannickal, Neinhuis, & Siegel, 2009). However, the detailed mapping and nuclear parcellation of orexinergic neurons has not been undertaken in other species of catarrhine (apes and Old World monkeys) or platyrrhine (New World

monkeys) primates, although the presence of these neurons has been noted and quantified in *Macaca mulatta* (e.g., Downs et al., 2007; Luna, Brown, Eghlidi, Kohama, & Urbanski, 2017).

In mammals orexinergic neurons are primarily found within the hypothalamus and are typically organized into three distinct clusters: (a) a main cluster in the perifornical area; (b) a zona incerta cluster in the dorsal lateral hypothalamus; and (c) an optic tract cluster of the ventrolateral hypothalamus (e.g., Calvey et al., 2015; Dell et al., 2013; Nixon & Smale, 2007). For the most part, these three clusters are similar across mammals, although variations in neuronal numbers and the complement of clusters have been observed (Davimes et al., 2017; Dell et al., 2012, 2013, 2016,b,c; Kruger et al., 2010; Malungo et al., 2020; Maseko, Patzke, Fuxe, & Manger, 2013). Despite the relatively small population of hypothalamic orexinergic neurons, the axons that emanate from these neurons project extensively throughout the central nervous system (CNS), forming variable densities of terminal networks in different regions of the brain (e.g., Calvey et al., 2015; Chen, Dun, Kwok, Dun, & Chang, 1999; Dell et al., 2013; Gravett et al., 2011; Zhang et al., 2002). Employing orexin-A immunocytochemistry, we describe the location and distribution of the orexinergic neurons and high-density terminal networks in the brains of a lar gibbon (*Hylobates lar*) and a chimpanzee (*Pan troglodytes*), as well as provide a stereological analysis of orexinergic neuronal numbers and somal volumes.

2 | MATERIALS AND METHODS

2.1 | Specimens

Brains from two healthy adult apes, a male lar gibbon (*H. lar*) (body mass: 5.5 kg, brain mass: 112 g, 5.5 years old) and a female chimpanzee (*P. troglodytes*) (body mass: 47 kg, brain mass: 388.1 g, 21 years old), were obtained from the Copenhagen Zoo, Denmark, and the Borås Zoo, Sweden, respectively. Both animals were born in captivity and showed no behavioral problems or stereotypies indicative of any neurological impairments. The animals were treated and used according to the guidelines of the University of Witwatersrand Animal Ethics Committee (Clearance number 2017/010/73/O), which correspond with those of the NIH for care and use of animals in scientific experimentation. The brains were obtained after the animals had been euthanized with sodium pentobarbital (i.v.), in line with population management decisions of the zoos independent of the current study (Bertelsen, 2018). Following euthanasia, the carotid arteries were cannulated, and the heads were perfused with an initial rinse of 0.9% saline solution at a temperature of 4°C followed by 4% paraformaldehyde in 0.1 M phosphate buffer (PB) at 4°C. The brains, which showed no signs of neuropathology, were removed from the skull and postfixed in 4% paraformaldehyde in 0.1 M PB (48 hr at 4°C) and allowed to equilibrate in 30% sucrose in 0.1 M PB before being stored in an antifreeze solution at −20°C until use (Manger et al., 2009).

2.2 | Sectioning and immunostaining

The brains were allowed to equilibrate in 30% sucrose in 0.1 M PB, and then frozen in crushed dry ice. The frozen brains were mounted to an aluminum stage and coronal sections

of 50 μm thickness were cut using a sliding microtome. Both brains were sectioned into 1 in 20 series, of which three series were used in the current study. The remaining 17 series were placed in antifreeze solution and stored at −20°C for later use. The three series used in this study were stained for Nissl, myelin, and immunostained for orexin-A (see below). Sections used for Nissl staining were mounted on 1% gelatine coated glass slides, cleared in a solution of 1:1 chloroform and 100% alcohol overnight, after which the sections were stained with 1% cresyl violet. The myelin series sections were refrigerated for 2 weeks in 5% formalin then mounted on 2% gelatine coated slides and stained with a modified silver stain (Gallyas, 1979). The Nissl and myelin stained sections were used to define the architecture of the hypothalamus and surrounding structures.

The series of sections used for orexin-A immunohistochemistry were initially treated for 30 min with an endogenous peroxidase inhibitor (49.2% methanol: 49.2% 0.1 M PB: 1.6% of 30% H_2O_2), followed by three 10 min rinses in 0.1 M PB. The sections were then preincubated at room temperature for 3 hr in a blocking buffer solution comprised of 3% normal goat serum, 2% bovine serum albumin (BSA, Sigma) and 0.25% Triton X-100 (Merck) in 0.1 M PB. The sections were then placed in a primary antibody solution (blocking buffer with appropriately diluted primary antibody) and incubated at 4°C for 48 hr under gentle shaking. To identify orexin-A containing cells bodies and axonal terminal networks, we used the AB3704 anti-Orexin-A rabbit polyclonal antibody from Merck-Millipore (AB3704, Merck-Millipore; RRID AB_91545; raised against a synthetic peptide corresponding to the c-terminal portion of bovine orexin-A peptide) at a dilution of 1:3000. The pattern of staining of orexinergic neurons in the hypothalamus and projections throughout the brain was similar to that seen in other mammals (e.g., Li & Kiruoac, 2008).

The incubation in the primary antibody solution was followed by three 10 min rinses in 0.1 M PB, after which the sections were incubated in a secondary anti-rabbit antibody solution for 2 hr at room temperature. The secondary antibody solution contained a 1:1,000 dilution of biotinylated anti-rabbit IgG (BA-1000, Vector Labs) in a solution containing 3% NGS and 2% BSA in 0.1 M PB. This was followed by three 10 min rinses in 0.1 M PB after which the sections were incubated in AB solution (Vector Labs) for 1 hr. After three further 10 min rinses in 0.1 M PB, the sections were placed in a solution of 0.05% diaminobenzidine in 0.1 M PB for 5 min, followed by the addition of 3 μl of 30% H_2O_2 to each 1 ml of solution in which each section was immersed. Chromatic precipitation of the sections was monitored visually under a low power stereomicroscope. This process was allowed to continue until the background staining of the sections was appropriate for architectonic analysis without obscuring any immunopositive structures. The precipitation process was stopped by immersing the sections in 0.1 M PB and then rinsing them twice more in 0.1 M PB. To check for nonspecific staining from the immunohistochemistry protocol, we omitted the primary antibody and the secondary antibody in selected sections, which produced no evident staining. The immunohistochemically stained sections were mounted on 1% gelatine coated slides and left to dry overnight. The sections were then dehydrated in graded series of alcohols, cleared in xylene and cover slipped with Depex.

2.3 | Stereological analysis

To quantify the total numbers of orexinergic neurons in the lar gibbon and chimpanzee hypothalamus, an unbiased design based systematic random sampling stereological protocol was employed. We used a MicroBrightfield (MBF) (Colchester, Vermont) system with a three-plane motorized stage, Zeiss.Z2 Axio Imager Vario microscope and StereoInvestigator software (MBF, version 11.08.1; 64-bit). Initially pilot studies were conducted to optimize sampling parameters, such as the counting frame and sampling grid sizes, and achieve a coefficient of error (CE) below 0.1 (Dell, Patzke, Spocter, Siegel, & Manger, 2016; Gundersen, 1988; West, Slomianka, & Gundersen, 1991). In addition, we measured the tissue section thickness at every sampling site and the vertical guard zone, at both the top and bottom of the section, was determined according to tissue thickness to avoid errors/biases due to sectioning artifacts (Dell, Patzke, Spocter, Siegel, & Manger, 2016; West et al., 1991), all undertaken using a 40× objective. Table 1 provides a detailed summary of the stereological parameters employed in the current study. To estimate the total number of orexinergic neurons, we used the optical fractionator probe (Dell, Patzke, Spocter, Siegel, & Manger, 2016; West et al., 1991), first estimating the total number within the right hypothalamus, and then doubling this estimate to obtain the total number of orexinergic neurons. To determine orexinergic neuronal volumes, we used the nucleator probe, with five rays being sampled in each probe. For all tissue sampled this probe was used concurrently with the optical fractionator while maintaining strict criteria, that is, only neurons with complete cell bodies were counted.

3 | RESULTS

As is typical of the orexinergic system, in both species of apes the neurons immunopositive to the orexin-A antibody used in the current study (OxA+ neurons) were found mostly within the hypothalamus. Within the hypothalamus, these neurons were arranged in three distinct clusters: (a) the main cluster; (b) the zona incerta cluster; and (c) the optic tract cluster (all three of which are typically observed across mammals), but it appears that there is an extended distribution of optic tract cluster neurons into the anterior ventromedial tuberal region of the hypothalamus (Figures 1–3). The OxA+ neurons gave rise to axons that formed terminal fields throughout the brain, but the densities of these terminal networks varied in the different regions. The distribution of both OxA+ neurons and terminal networks was very similar in the two species studied, thus the following description applies to both species unless otherwise noted.

3.1 | Distribution and morphology of orexinergic neurons

OxA+ neurons were found predominantly within the hypothalamus of both species. Within the hypothalamus, these neurons were found from close to the midline across to the lateral edge, and from the most ventral to the most dorsal portions of the hypothalamus (Figures 1–3). Typically in mammals the OxA+ neurons have been parcellated into three distinct clusters, a main cluster which houses the majority of the OxA+ neurons in the perifornical region, a zona incerta cluster in the dorsolateral aspect of the hypothalamus and an optic tract cluster in the ventrolateral aspect of the hypothalamus (e.g., Calvey et al., 2015; Dell et al., 2013; Nixon & Smale, 2007). In both ape species these three clusters of OxA+

neurons were clearly evident (Figures 1–5). As is typical for mammals, the main cluster comprised the majority of OxA+ neurons in the regions surrounding the passage of the fornix through the hypothalamus (Figures 1d–f, 2, 3). Extending dorsolaterally from this main cluster, a small number of OxA+ neurons were observed in the dorsal lateral aspect of the hypothalamus forming the zona incerta cluster (Figures 1d–f, 2, 3). These cells were most evident in the portion of the hypothalamus adjacent to the medial border of the zona incerta, with a few cells being located outside the hypothalamus, in the white matter immediately dorsomedial to the zona incerta (Figures 1–3). Extending ventrolaterally from the main cluster, a small number of OxA+ neurons were observed in the ventrolateral hypothalamus adjacent to the optic tract, these neurons being the optic tract cluster (Figures 1b–f, 2, 3). Interestingly, and in contrast to all other mammals previously studied including strepsirrhine primates (Calvey et al., 2015), a small number of OxA+ neurons were observed in the anterior ventromedial portion of the hypothalamus, in what we broadly define as the tuberal region. These cells were found above the optic chiasm, bordering the ventrolateral margin of the third ventricle (Figures 1a–e, 2b,c, 3b). As this is a novel region of the hypothalamus to contain OxA+ neurons, and that these neurons appear contiguous with the "standard" optic tract cluster, we have termed these neurons the optic tract cluster extension.

While in some species, such as the elephant and cetartiodactyls (Davimes et al., 2017; Dell et al., 2016,b,c; Malungo et al., 2020; Maseko et al., 2013), there are differences in the morphology of orexinergic neurons in different parts of the hypothalamus, in both species of ape studied, the morphology of the OxA+ neurons in the three different clusters and the extension was very similar. The majority of these neurons were bipolar, but a noticeable proportion of these neurons were multipolar, especially in the main cluster. In the main cluster, optic tract cluster and extension, the dendrites emanating from these neurons showed no consistent orientation (Figures 4 and 5); however, the OxA+ neurons of the zona incerta cluster had dendrites that were oriented in a plane parallel to the upper border of the zona incerta (Figures 4b and 5b).

3.2 | Numbers and soma volumes of orexinergic neurons

As there was no distinct difference in the overall cell morphology between the clusters of orexinergic neurons (see above, but also see Maseko et al., 2013; Dell et al., 2016,b,c; Davimes et al., 2017; Malungo et al., 2020, where clear differences in soma size exist in the orexinergic neurons in elephants and cetartiodactyls), we estimated total orexinergic neurons numbers stereologically rather than quantify them as individual clusters. Within the hypothalamus of the lar gibbon, we estimated a total of 52,576 OxA+ neurons (CE, Gundersen $m = 1, 0.08$), while in the chimpanzee we estimated a total of 107,396 OxA+ neurons (CE, Gundersen $m = 1, 0.09$). Thus, the larger-brained chimpanzee (brain mass = 388.1 g) presented with substantially more OxA+ neurons than the smaller-brained lar gibbon (brain mass = 112 g). The median cell volume of the OxA+ neurons in the hypothalamus of the lar gibbon was 4,664 μm^3 (CE = 0.003), while in the chimpanzee this median was 5,926 μm^3 (CE = 0.004). Thus, the volume of the OxA+ neuronal soma was substantially larger in the chimpanzee compared to the lar gibbon.

3.3 | Orexinergic terminal networks

OxA+ terminal networks were observed throughout the brains of both species studied, but the density of these terminal networks varied substantially between brain regions. These terminal networks were comprised of axons evincing *boutons en passant*, and as previously described in cetartiodactyls (Dell et al., 2015), both large and small boutons were observed on the terminal segments of the OxA+ axons. While not quantified, the number of small orexinergic boutons clearly outnumber the large boutons, as seen in the cetartiodactyls (Dell et al., 2015), and the proportions observed in cetartiodactyls appears to be reflected in the brains of both ape species studied. This proportion of OxA+ boutons was observed throughout all regions of the brain, regardless of variation in terminal network densities (Figures 4–8).

High density OxA+ terminal networks were observed throughout the entire hypothalamus (Figures 4 and 5), both in the regions where the OxA+ neurons were observed and in surrounding regions. The midline and intralaminar nuclei of the dorsal thalamus also showed high density OxA+ terminal networks (Figure 6), and, to an extent, provide a distinct outline for these dorsal thalamic nuclear complexes. Within the midbrain and the pons, high density OxA+ terminal networks were observed in the regions corresponding to the serotonergic dorsal raphe nuclear complex (Figure 7a,b), and also in the locus coeruleus nuclear complex, specifically in the locus coeruleus proper within the periventricular gray matter, and in the compact portion of the subcoeruleus in the adjacent tegmentum, where in both regions there is a high density of noradrenergic neurons (Figure 7c,d, pers. obs.). The remaining regions of the brain had relatively lower densities of orexinergic boutons, with the OxA terminal networks in cerebral cortex and dorsal striatopallidal complex being clear examples of regions with a low density of terminals (Figure 8).

4 | DISCUSSION

In this study we have provided an anatomical description of the orexinergic system in the brain of two apes, a lar gibbon and a chimpanzee. In general, the orexinergic system in the brains of the apes studied is very similar to that seen in other mammals, including humans. This similarity includes the location and parcellation of the orexinergic neurons in the hypothalamus, as well as the broad, but heterogeneous, projections of these neurons throughout the neuraxis and the presence of both large and small *boutons en passant* forming the orexinergic terminal networks. The one significant difference to other mammalian species is the presence of orexinergic neurons in the tuberal region of the ape hypothalamus, the extension of the optic tract cluster, which to a certain degree, is also present in the human hypothalamus. These findings are discussed in an evolutionary and functional context.

4.1 | Conserved features of the orexinergic system in mammals

The organization of the orexinergic system across mammals is, for the most part (but see below), quite consistent across mammals. The orexinergic neurons are primarily located within the hypothalamus (a few neurons are located within or adjacent to the zona incerta), and these neurons project throughout the neuraxis, with different regions having higher or lower densities of orexinergic terminal fields. In this sense, the apes studied closely resemble

other mammalian species, apart from the extension of the optic tract cluster of orexinergic neurons into the tuberal region of the hypothalamus. Despite this overall similarity, there are still characteristics of interest that require further detailed study to translate from commonly used animal models, such as laboratory rodents, to humans.

There is notable variation in the numbers of orexinergic neurons across species that have vastly different brain mass. Numbers of orexinergic neurons have been estimated for a range of mammalian species, including laboratory rat ($n \approx 4{,}000$, brain mass ≈ 2 g, Kilduff & Peyron, 2000), laboratory mouse ($n \approx 2{,}000$, brain mass ≈ 0.4 g, Brownell & Conti, 2010), domestic dog ($n \approx 30{,}000$, brain mass ≈ 100 g, Thannickal et al., 2000), giraffe ($n \approx 15{,}003$, brain mass ≈ 526.5 g, Dell et al., 2012), harbor porpoise ($n \approx 21{,}254$, brain mass ≈ 494.5 g, Dell et al., 2012), minke whale ($n = 277{,}604$, brain mass = 2,900 g; Dell, Karlsson, Patzke, Spocter, et al., 2016), river hippopotamus ($n = 68{,}398$, brain mass = 407.5 g, Dell, Patzke, Spocter, Bertelsen, et al., 2016), Arabian oryx ($n = 24{,}549$, brain mass = 166 g, Davimes et al., 2017), blue wildebeest ($n = 11{,}717$, brain mass = 390.1, Malungo et al., 2020), macaque monkey ($n \approx 48{,}000$, brain mass ≈ 90 g, Downs et al., 2007), lar gibbon ($n = 52{,}576$, brain mass = 112 g, current study), chimpanzee ($n = 107{,}396$, brain mass = 388.1 g, current study) and human ($n \approx 70{,}000$, brain mass ≈ 1,400 g, Thannickal, Moore, et al., 2000). What is clear is that the larger brains house more orexinergic neurons, but that this increase in neuronal numbers with increased brain mass is not a linear relationship and is likely to be a negative allometry (i.e., for every doubling in brain mass, the number of orexinergic neurons will increase by less than double). However, any allometric analysis needs to be cognizant of the phylogenetic relationships between the species being analyzed and the potential specializations of the orexinergic system, such as the parvocellular cluster in elephants and cetartiodactyls (Davimes et al., 2017; Dell et al., 2016,b,c; Malungo et al., 2020; Maseko et al., 2013), that may complicate the analysis and interpretation. At present there is not enough data from a broad enough range of species to warrant undertaking an allometric analysis.

The second characteristic of this system that would be important to understand across species, in terms of translational research, are the densities of orexinergic boutons in homologous brain regions in different species, and the relative proportions of the large and small boutons across species. It would be important to understand whether orexinergic bouton densities scale with neuronal numbers, nonneuronal numbers, or with structure volume/mass. In addition, it appears that in all species studied (including humans, see Figure 9), the orexinergic *boutons en passant* are of two types, large and small. In cetartiodactyls, the relative proportion of large and small orexinergic boutons in the terminal networks of the cerebral cortex appears to be quite stable across species and brain masses (Dell et al., 2015); however, the proportions of these boutons in different brain regions has not been examined in the same species, or in homologous brain regions across species (apart from cetartiodactyls). Given that it is likely that the larger boutons are drivers of postsynaptic activity, while the smaller boutons are modulators of postsynaptic activity (Sherman & Guillery, 1998), potentially acting through volume transmission (Fuxe et al., 2010), a deeper understanding of this potential variation and how it may change with brain size and phylogenetic affinities may provide important insights into the function of this system.

Understanding whether there are specific scaling laws that predict the numbers of orexinergic neurons in the brain of mammalian species, or bouton densities in various parts of the mammalian brain, or variations in the relative proportion of small and large orexinergic boutons, would be very important in understanding the potential effects and dose requirements of specific pharmaceuticals that may be developed in future to address dysfunctions of this system, such as seen in narcolepsy (e.g., Thannickal et al., 2009; Thannickal, Moore, et al., 2000).

4.2 | A novel cluster of orexinergic neurons in apes? Evolutionary considerations

As detailed above, the majority of the features of the orexinergic system observed in the two ape species studied are very similar to that observed across the majority of mammals. Nonetheless, the presence of orexinergic neurons in the tuberal region of the ape hypothalamus, the extension of the optic tract cluster, has not yet been explicitly reported in any mammal species studied. Across the breadth of mammalian phylogeny there is variation in the complement of orexinergic clusters present in the hypothalamus. For example, the optic tract cluster is not observed in microchiropteran bats (Kruger et al., 2010, although it is present in megachiropteran bats, Dell et al., 2013), while in the African elephant and cetartiodactyls (giraffe, Arabian oryx, blue wildebeest, river hippopotamus, harbor porpoise, minke whale), a medially located parvocellular cluster is observed (Davimes et al., 2017; Dell et al., 2012, 2016,c; Malungo et al., 2020; Maseko et al., 2013). However, the parvocellular cluster of orexinergic neurons in the elephant and cetartiodactyls is not equivalent to the optic tract cluster extension observed in the lar gibbon and chimpanzee, as these neurons in apes show the same morphology as the orexinergic neurons in the other hypothalamic clusters, while those of the parvocellular cluster in the elephant and cetartiodactyls are distinctly smaller than those observed in the main, zona incerta and optic tract clusters.

In primates, the only species in which the distribution and parcellation of orexinergic neurons has been provided in detail are three strepsirrhines (*Galago demidoff, Perodicticus potto* and *Lemur catta*) (Calvey et al., 2015) and humans (e.g., Thannickal et al., 2009; Thannickal, Moore, et al., 2000), although photomicrographs appear to show a similar organization in the macaque monkey (e.g., Downs et al., 2007; Luna et al., 2017). In these primates, the main, zona incerta and optic tract clusters were reported, but the optic tract cluster extension was not observed in these studies (see Figure 9 for an example of orexinergic immunostaining in the human hypothalamus). In contrast, in one study of humans using in situ hybridization directed against the orexin mRNA, expression was observed in neurons in the optic tract cluster extension in addition to the other regions of the hypothalamus where immunohistochemistry typically reveals orexinergic neurons (Krolewski et al., 2010, see their Figures 1f and 2f). Thus, in primates we have the unusual situation where there do not appear to be orexinergic neurons in the optic tract cluster extension of the tuberal region in strepsirrhines, while the orexin gene is expressed in this region of the human hypothalamus but does not appear to lead to the production of the orexin neuropeptide. In contrast, in the lar gibbon and chimpanzee, one would assume, given the immunolocalization of orexinergic neurons in the optic tract cluster extension of the tuberal region, that the orexin gene is also expressed in some of the neurons of this

region. Thus, at present, we can conclude that an optic tract cluster extension in the tuberal region is likely to be a shared feature of the Hominoidea (apes, including humans), but that this cluster appears to have become nonfunctional in humans. However, this conclusion must be reached tentatively, as the primary orexin-A antibody used in the current study is different to that used in the study of the human (Thannickal, Moore, et al., 2000), thus the disparate findings may be the result of different binding sites on the orexin neuropeptide for each antibody. In addition, it has to be noted that in mammals the relationship between protein expression and mRNA concentrations usually does not exceed 40% (Abreu, Penalva, Marcotte, & Vogel, 2009), which may provide some explanation as to the disparate results between the lar gibbon and chimpanzee compared to the human as reported here.

Whether this optic tract cluster extension of the tuberal region is a derived feature of the hypothalamus of the Hominoidea not shared by other primates remains to be determined, as detailed mapping studies of orexinergic neurons in other primates (Tarsiformes—tarsiers, Platyrrhini—New World monkeys, and Cercopithecoidea—Old World monkeys) are required to reveal the full extent of the phylogenetic occurrence of this potentially novel orexinergic cluster. The outcome of such studies will be important in determining the confidence with which functional studies of the orexinergic system in laboratory rodents can be translated to humans, and will be instructive in the prediction of potential side-effects that the administration of medicinal pharmaceuticals targeting the orexinergic system developed and tested in laboratory rodents may have on humans. Given the importance of the orexinergic system in relation to ailments such as narcolepsy (Thannickal et al., 2009; Thannickal, Moore, et al., 2000) and addiction (Thannickal et al., 2018), understanding the similarities and variances between model species and human targets is important.

4.3 | Potential functions of the optic tract cluster extension

Identifying this novel cluster of orexinergic neurons within the ape hypothalamus, and the unusual features of the neurons potentially forming this cluster in humans, is of interest, as it raises the question of what potential functions these neurons might subserve. Because it is not possible to record from and determine the precise anatomy and connectivity of these neurons in apes and humans, direct insights about function are limited. The postsynaptic action of orexin is, in general, excitatory (e.g., Bayer et al., 2004; Chrobok, Palus-Chramiec, Chrzanowska, Kepczynski, & Lewandowski, 2017) and this excitation acts in a chronologically relevant manner (Azeez, del Gallo, Cristino, & Bentivoglio, 2018). However, the projection patterns of orexinergic neurons are often diffuse, spreading across much of the neuraxis (e.g., Peyron et al., 1998), although given the high density of orexinergic terminal networks within the hypothalamus, it would appear that they also project locally. This indicates the possibility that these optic tract cluster extension orexinergic neurons in the ape hypothalamus, may provide a stronger excitatory influence on the neurons located in the supraoptic and tuberal regions of the hypothalamus than would be the case if these neurons were not present. The neurons within the anterior and supraoptic regions of the hypothalamus are involved in a variety of functions, including blood pressure control and water balance, thermoregulation, eating, reproduction, daily rhythms, stress and metabolic control, and sleep and arousal (e.g., Pop, Crivii, & Opincariu, 2018). It is difficult to determine whether enhanced excitation of the neurons subserving these functions by optic

tract cluster extension orexinergic neurons would have a great influence on their function, but it is possible that even the smallest functional augmentation of the neurons in the supraoptic and tuberal regions of the hypothalamus may have a significant effect. At present further discussion regarding the potential functional attributes and correlates of these optic tract cluster extension orexinergic neurons awaits further study.

ACKNOWLEDGMENT

The Leakey Foundation (PRM, CCS), and the National Research Foundation of South Africa (PRM).

Funding information

Leakey Foundation; National Research Foundation of South Africa

DATA AVAILABILITY STATEMENT

Data have not been shared due to this study being primarily an observational study on histological slides.

Abbreviations:

3V	third ventricle
4V	fourth ventricle
A6	locus coeruleus nuclear complex
A7	subcoeruleus nuclear complex
A9m	substantia nigra, medial division
ac	anterior commissure
acp	anterior commissure, posterior part
Amyg	amydaloid body
ca	cerebral aqueduct
Diag.B	diagonal band of Broca
DRd	dorsal raphe nucleus, dorsal part
DRl	dorsal raphe nucleus, lateral part
DRp	dorsal raphe nucleus, peripheral part
DRv	dorsal raphe nucleus, ventral part
DT	dorsal thalamus
F	fornix
GPe	globus pallidus, external part

GPi	globus pallidus, internal part
HyN	hypophysis, pars nervosa
ic	internal capsule
IH	infundibular hypothalamic nucleus
Is.C	island of Calleja
LPO	lateral preoptic area
MB	mammillary bodies
Mc	main cluster of orexinergic neurons
me5	tract of the fifth mesencephalic nucleus
mmt	mammillothalamic tract
MnPO	median preoptic nucleus
MPA	medial preoptic area
N.Bas	nucleus basalis
NSt	nigrostriatal tracte
OC	optic chiasm
OT	optic tract
OTc	optic tract cluster of orexinergic neurons
OTce	extension of optic tract cluster of orexinergic neurons
P	putamen nucleus
Para	anterior paraventricular nucleus of the thalamus
PC	cerebral peduncle
PHA	posterior hypothalamic area
R	thalamic reticular nucleus
SNR	substantia nigra, reticular part
SON	supraoptic nucleus
ST	stria terminalis
STN	subthalamic nucleus
TO	olfactory tubercle
VMH	ventromedial hypothalamic nucleus

VP	ventral pallidum
zi	zona incerta
Zic	zona incerta cluster of orexinergic neurons

REFERENCES

Abreu R. d. S., Penalva LO, Marcotte EM, & Vogel C (2009). Global signature of protein and mRNA expression levels. Molecular BioSystems, 5, 1512–1526. 10.1039/B9083165D [PubMed: 20023718]

Azeez IA, del Gallo F, Cristino L, & Bentivoglio M (2018). Daily fluctuation of orexin neuron activity and wiring: The challenge of "chronoconnectivity". Frontiers in Pharmacology, 9, 1061. 10.3389/fphar.2018.01061 [PubMed: 30319410]

Bayer L, Serafin M, Eggerman E, Saint-Mleux B, Machard D, Jones BE, & Muhlethaler M (2004). Exclusive postsynaptic action of hypocretin-orexin on sublayer 6b cortical neurons. Journal of Neuroscience, 24, 6760–6764. 10.1523/JNEUROSCI.1783-04.2004 [PubMed: 15282280]

Bertelsen MF (2018). Issues surrounding surplus animals in zoos. In Miller RE, Lamberski N, & Calle P (Eds.), Fowler's zoo and wild animal medicine, current therapy (Vol. 9, pp. 134–137). St. Louis, MO: Elsevier.

Brownell SE, & Conti B (2010). Age- and gender-specific changes of hypocretin immunopositive neurons in C57Bl/6 mice. Neuroscience Letters, 472, 29–32. 10.1016/j.neulet.2010.01.048 [PubMed: 20117171]

Calvey T, Patzke N, Kaswera-Kyamayaka C, Gilissen E, Bertelsen MF, Pettigrew JD, & Manger PR (2015). Organization of cholinergic, catecholaminergic, serotonergic and orexinergic nuclei in three strepsirrhine primates: *Galago demidoff, Perodicticus potto and Lemur catta*. Journal of Chemical Neuroanatomy, 20, 42–57. 10.1016/j.jchemneu.2015.10.007

Chen CT, Dun SL, Kwok EH, Dun NJ, & Chang JK (1999). Orexin-A like immunoreactivity in the rat brain. Neuroscience Letters, 260, 161–164. 10.1016/s0304-3940(98)00977-x [PubMed: 10076892]

Chow M, & Cao M (2016). The hypocretin/orexin system in sleep disorders: Preclinical insights and clinical progress. Nature and Science of Sleep, 8, 81–86. 10.2147/NSS.S76711

Chrobok L, Palus-Chramiec K, Chrzanowska A, Kepczynski M, & Lewandowski MH (2017). Multiple excitatory actions of orexins upon thalamo-cortical neurons in dorsal lateral geniculate nucleus—Implications for vision modulation by arousal. Scientific Reports, 7, 7713. 10.1038/s41598-017-08202-8 [PubMed: 28794459]

Davimes JG, Alagaili AN, Bennett NC, Mohammed OR, Bhagwandin A, Manger PR, & Gravett N (2017). Neurochemical organization and morphology of the sleep related nuclei in the brain of the Arabian oryx, *Oryx leucoryx*. Journal of Chemical Neuroanatomy, 81, 53–70. 10.1016/j.jchemneu.2017.02.002 [PubMed: 28163217]

de Lecea L, Kilduff TS, Peyron C, Gao XB, Foye PE, Danielson PE, … Sutcliffe JG (1998). The hypocretins: Hypothalamus-specific peptides with neuroexcitatory activity. Proceedings of the National Academy of Sciences of the United States of America, 95, 322–327. 10.1073/pnas.95.1.322 [PubMed: 9419374]

de Lecea L, & Sutcliffe JG (2005). The hypocretins and sleep. The FEBS Journal, 272, 5675–5688. 10.1111/j.1742-4658.2005.04981.X [PubMed: 16279933]

Dell LA, Karlsson KÆ, Patzke N, Spocter MA, Siegel JM, & Manger PR (2016). Organization of the sleep-related neural systems in the brain of the minke whale (*Balaenoptera acutorostrata*). Journal of Comparative Neurology, 524, 2018–2035. 10.1002/cne.23931

Dell LA, Kruger JL, Pettigrew JD, & Manger PR (2013). Cellular location and major terminal networks of the orexinergic system in the brain of two megachiropterans. Journal of Chemical Neuroanatomy, 53, 64–71. 10.1016/j.jchemneu.2013.09.001 [PubMed: 24041616]

Dell LA, Patzke N, Bhagwandin A, Bux F, Fuxe K, Barber G, … Manger PR (2012). Organization and number of orexinergic neurons in the hypothalamus of two species of Cetartiodactyla: A comparison of giraffe (*Giraffe camelopardalis*) and harbour porpoise (*Phocoena phocoena*).

Journal of Chemical Neuroanatomy, 44, 98–109. 10.1016/jyjchemneu.2012.06.001 [PubMed: 22683547]

Dell LA, Patzke N, Spocter MA, Bertelsen MF, Siegel JM, & Manger PR (2016). Organization of the sleep-related neural systems in the brain of the river hippopotamus (*Hippopotamus amphibius*). Journal of Comparative Neurology, 524, 2036–2058. 10.1002/cne.23930

Dell LA, Patzke N, Spocter MA, Siegel JM, & Manger PR (2016). Organization of the sleep-related neural systems in the brain of the harbour porpoise (*Phocoena phocoena*). Journal of Comparative Neurology, 524, 1999–2017. 10.1002/cne.23929

Dell LA, Spocter MA, Patzke N, Karlsson KÆ, Alagaili AN, Bennett NC, … Manger PR (2015). Orexinergic bouton density is lower in the cerebral cortex of cetaceans compared to artiodactyls. Journal of Chemical Neuroanatomy, 68, 61–76. 10.1016/jjchemneu.2015.07.007 [PubMed: 26232521]

Downs JL, Dunn MR, Borok E, Shanabrough M, Horvath TL, Kohama SG, & Urbanski HF (2007). Orexin neuronal changes in the locus coeruleus of the aging rhesus macaque. Neurobiology of Aging, 28, 1286–1295. 10.1016/j.neurobiolaging.2006.05.025 [PubMed: 16870307]

Elias CF, Saper CB, Maratos-Flier E, Tritos NA, Lee C, Kelly J, … Elmquist JK (1998). Chemically defined projections linking the mediobasal hypothalamus and the lateral hypothalamic area. Journal of Comparative Neurology, 402, 442–459. 10.1002/(SICI)1096-9861(19981228)402:4<442::AID-CNE2>3.0.CO;2-R

Fuxe K, Dahlström AB, Jonsson G, Marcellino D, Guescini M, Dam M, … Agnati L (2010). The discovery of central monoamine neurons gave volume transmission to the wired brain. Progress in Neurobiology, 90, 82–100. 10.1016/j.pneurobio.2009.10.012 [PubMed: 19853007]

Gallyas F (1979). Silver staining of myelin by means of physical development. Neurological Research, 1, 203–209. 10.1080/01616412.1979.11739553 [PubMed: 95356]

Gravett N, Bhagwandin A, Fuxe K, & Manger PR (2011). Distribution of orexin-A immunoreactive neurons and their terminal networks in the brain of the rock hyrax, *Procavia capensis*. Journal of Chemical Neuroanatomy, 41, 86–96. 10.1016/j.jchemneu.2010.11.005 [PubMed: 21126575]

Gundersen HJ (1988). The nucleator. Journal of Microscopy—Oxford, 151, 3–21. 10.1111/j.1365-2818.1988.tb04609.x

Iqbal J, Pompolo S, Sakurai T, & Clarke IJ (2001). Evidence that orexin-containing neurones provide direct input to gonadotropin-releasing hormone neurones in the ovine hypothalamus. Journal of Neuroendocrinology, 13, 1033–1041. 10.1046/j.1365-2826.2001.00719.x [PubMed: 11722699]

Khorooshi RMH, & Klingenspor M (2005). Neuronal distribution of melanin-concentrating hormone, cocaine- and amphetamine-regulated transcript and orexin B in the brain of the Djungarian hamster (*Phodopus sungorus*). Journal of Chemical Neuroanatomy, 29, 137–148. 10.1016/j.jchemneu.2004.10.003 [PubMed: 15652700]

Kilduff TS, & Peyron C (2000). The hypocretin/orexin ligand-receptor system: Implication for sleep and sleep disorders. Trends in Neuroscience, 23, 359–365. 10.1016/S0166-2236(00)01594-0

Krolewski DM, Medina A, Kerman IA, Bernard R, Burker S, Thompson RC, … Watson SJ (2010). Expression patterns of corticotropin-releasing factor, arginine vasopressin, histidine decarboxylase, melanin-concentrating hormone, and orexin genes in the human hypothalamus. Journal of Comparative Neurology, 518, 4591–4611. 10.1002/cne.22480

Kruger JL, Dell LA, Pettigrew JD, & Manger PR (2010). Cellular location and major terminal networks of the orexinergic system in the brains of five microchiropteran species. Journal of Chemical Neuroanatomy, 40, 256–262. 10.1016/jjchemneu.2010.07.004 [PubMed: 20654711]

Li S, & Kiruoac J (2008). Projections from the paraventricular nucleus of the thalamus to the forebrain, with special emphasis on the extended amygdala. Journal of Comparative Neurology, 506, 263–287. 10.1002/cne.21502

Luna SL, Brown DI, Eghlidi DH, Kohama SG, & Urbanski HF (2017). Locomotor activity and the expression of orexin A and orexin B in aged female rhesus macaques. Neurobiology of Aging, 50, 1–4. 10.1016/j.neuroioaging.2016.10.016 [PubMed: 27837674]

Mai JK, Paxinos G, & Assheuer J (2004). Atlas of the human brain (3rd ed.). New York, NY: Academic Press.

Malungo IB, Gravett N, Bhagwandin A, Davimes JG, & Manger PR (2020). A preliminary description of the sleep-related neural systems in the brain of the blue wildebeest, *Connochaetes taurinus*. The Anatomical Record, 10, 142–152. 10.1002/ar.24265

Manger PR, Pillay P, Maseko BC, Bhagwandin A, Gravett N, Moon DJ, … Hemingway J (2009). Acquisition of brains from the African elephant (*Loxodonta africana*): Perfusion-fixation and dissection. Journal of Neuroscience Methods, 179, 16–21. 10.1016/j7jneumeth.2009.01.001 [PubMed: 19168095]

Maseko BC, Patzke N, Fuxe K, & Manger PR (2013). Architectural organization of the African elephant diencephalon and brainstem. Brain, Behavior and Evolution, 82, 83–128. 10.1159/000352004

Moore RY, Abrahamson EA, & van den Pol A (2001). The hypocretin neuron system: An arousal system in the human brain. Archives Italiennes Biologie, 139, 195–205.

Nishino S, Ripley B, Overeem S, Lammers GJ, & Mignot E (2000). Hypocretin (orexin) deficiency in human narcolepsy. The Lancet, 355, 39–40. 10.1016/S0140-6736(99)05582-8

Nixon JP, & Smale L (2007). A comparative analysis of the distribution of immunoreactive orexin a and B in the brains of nocturnal and diurnal rodents. Behavioral and Brain Functions, 3, 28. 10.1186/1744-9081-3-28 [PubMed: 17567902]

Peyron C, Faraco J, Rogers W, Ripley B, Overeem S, Charnay Y, … Mignot E (2000). A mutation in a case of early onset narcolepsy and a generalized absence of hypocretin peptides in human narcoleptic brains. Nature Medicine, 6, 991–997. 10.1038/79690

Peyron C, Tighe DK, van den Pol AN, de Lecea L, Heller HC, Sutcliffe JG, & Kilduff TS (1998). Neurons containing hypocretin (orexin) project to multiple neuronal systems. Journal of Neuroscience, 18, 9996–10015. 10.1523/JNEUROSCI.18-23-09996.1998 [PubMed: 9822755]

Pop MG, Crivii C, & Opincariu I (2018). Chapter 1. Anatomy and function of the hypothalamus. In Baloyannis S & Gordeladze J (Eds.), The hypothalamus in health and disease (pp. 3–14). London: IntechOpen. 10.5772/intechopen.80728

Sherman SM, & Guillery RW (1998). On the actions that one nerve cell can have on another: Distinguishing “drivers” from “modulators”. Proceedings of the National Academy of Sciences of the United States of America, 95, 7121–7126. 10.1073/pnas.95.12.7121 [PubMed: 9618549]

Thannickal TC, John J, Shan L, Swaab DF, Wu M-F, Ramanathan L, … Siegel JM (2018). Opiates increase the number of hypocretin-producing cells in mouse and human brain and reverse cataplexy in a mouse model of narcolepsy. Science Translational Medicine, 447, eaao4953. 10.1126/scitranslmed.aao4953

Thannickal TC, Moore RY, Nienhuis R, Ramanathan L, Gulyani S, Aldrich M, … Siegel JM (2000). Reduced number of hypocretin neurons in human narcolepsy. Neuron, 27, 469–474. 10.1016/s0896-6273(00)00058-1 [PubMed: 11055430]

Thannickal TC, Neinhuis R, & Siegel JM (2009). Localized loss of hypocretin (orexin) cells in narcolepsy without cataplexy. Sleep, 32, 993–998. 10.1093/sleep/32.8.993 [PubMed: 19725250]

Thannickal TC, Nienhuis R, Ramanathan L, Guliyani S, Turner K, Chestnut B, & Siegel JM (2000). Preservation of hypocretin neurons in genetically narcoleptic dogs. Sleep, 23, A296.

West MJ, Slomianka L, & Gundersen HJ (1991). Unbiased stereological estimation of the total number of neurons in the sub-divisions of the rat hippocampus using the optical fractionator. Anatomical Record, 231, 482–497. 10.1002/ar.1092310411

Yamamoto Y, McKinley MJ, Nakazato M, Yamashita H, Shirahata A, & Ueta Y (2006). Postnatal development of orexin-A and orexin-B like immunoreactivities in the Eastern grey kangaroo (*Macropus gigaenteus*) hypothalamus. Neuroscience Letters, 392, 124–128. 10.1016/j.neulet.2005.09.014 [PubMed: 16188385]

Zhang JH, Sampogna S, Morales FR, & Chase MH (2002). Co-localization of hypocretin-1 and hypocretin-2 in the cat hypothalamus and brainstem. Peptides, 23, 1479–1483. 10.1016/s0196-9781(02)00084-0 [PubMed: 12182950]

Zhang XY, Yu L, Zhuang QX, Zhu JN, & Wang JJ (2013). Central functions of the orexinergic system. Neuroscience Bulletin, 29, 355–365. 10.1007/s12264-012-1297-4 [PubMed: 23299718]

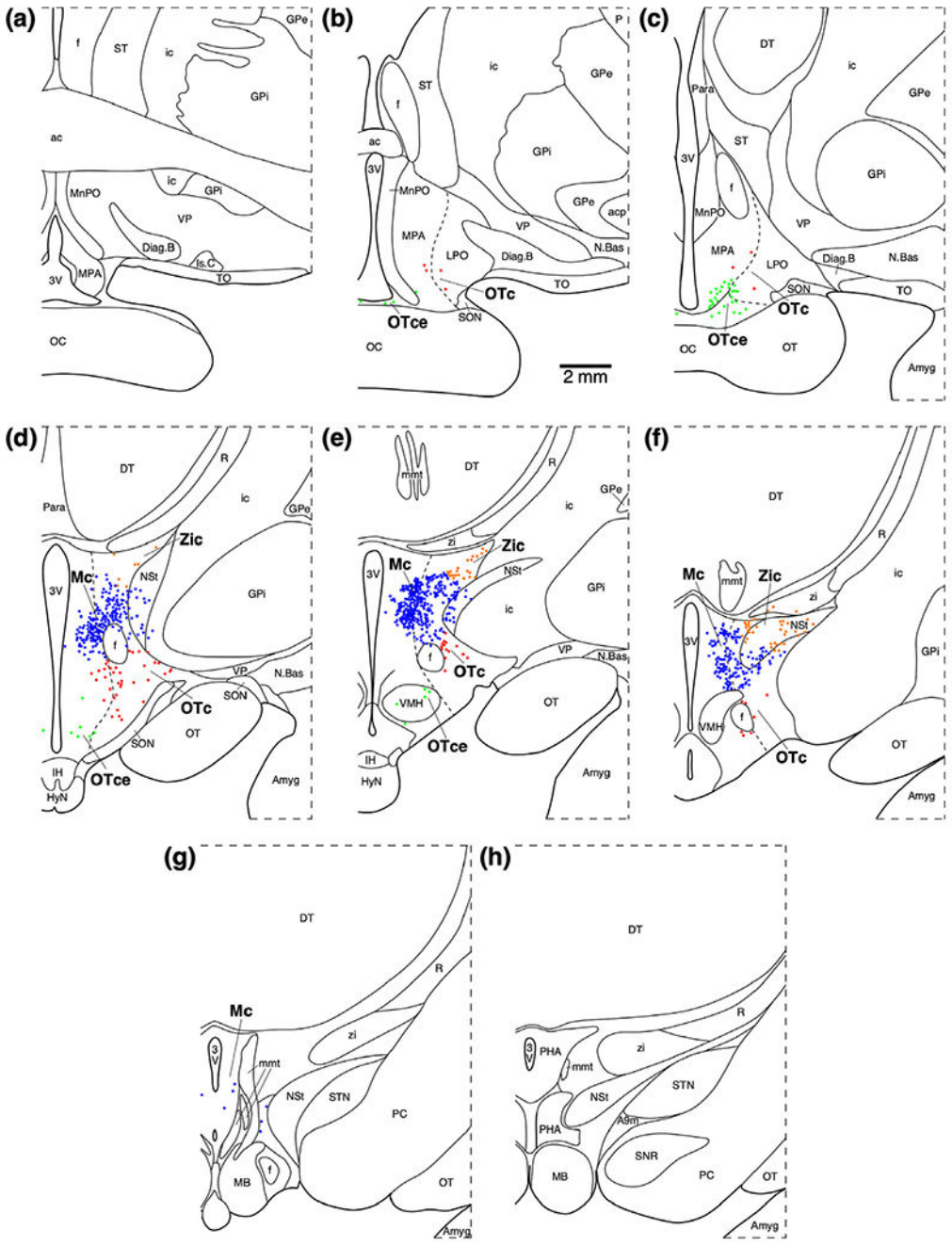

FIGURE 1.

Serial drawings of coronal sections through one half of the lar gibbon hypothalamus from the level of the decussation of the anterior commissure (ac) through to the mammillary bodies (MB). (a) is the most rostral section, (h) the most caudal. The architectural outlines were drawn using Nissl and myelin stains and orexinergic immunoreactive neurons marked on the drawings. The different colored dots represent individual orexinergic cluster, with each different color representing a specific nucleus or nuclear subdivision: Main cluster (Mc)—blue dots; zona incerta cluster (Zic)—orange dots; optic tract cluster (OTc)—red

dots; extension of the optic tract cluster (OTce)—green dots. The drawings are spaced approximately 1,000 μm apart. See list for abbreviations

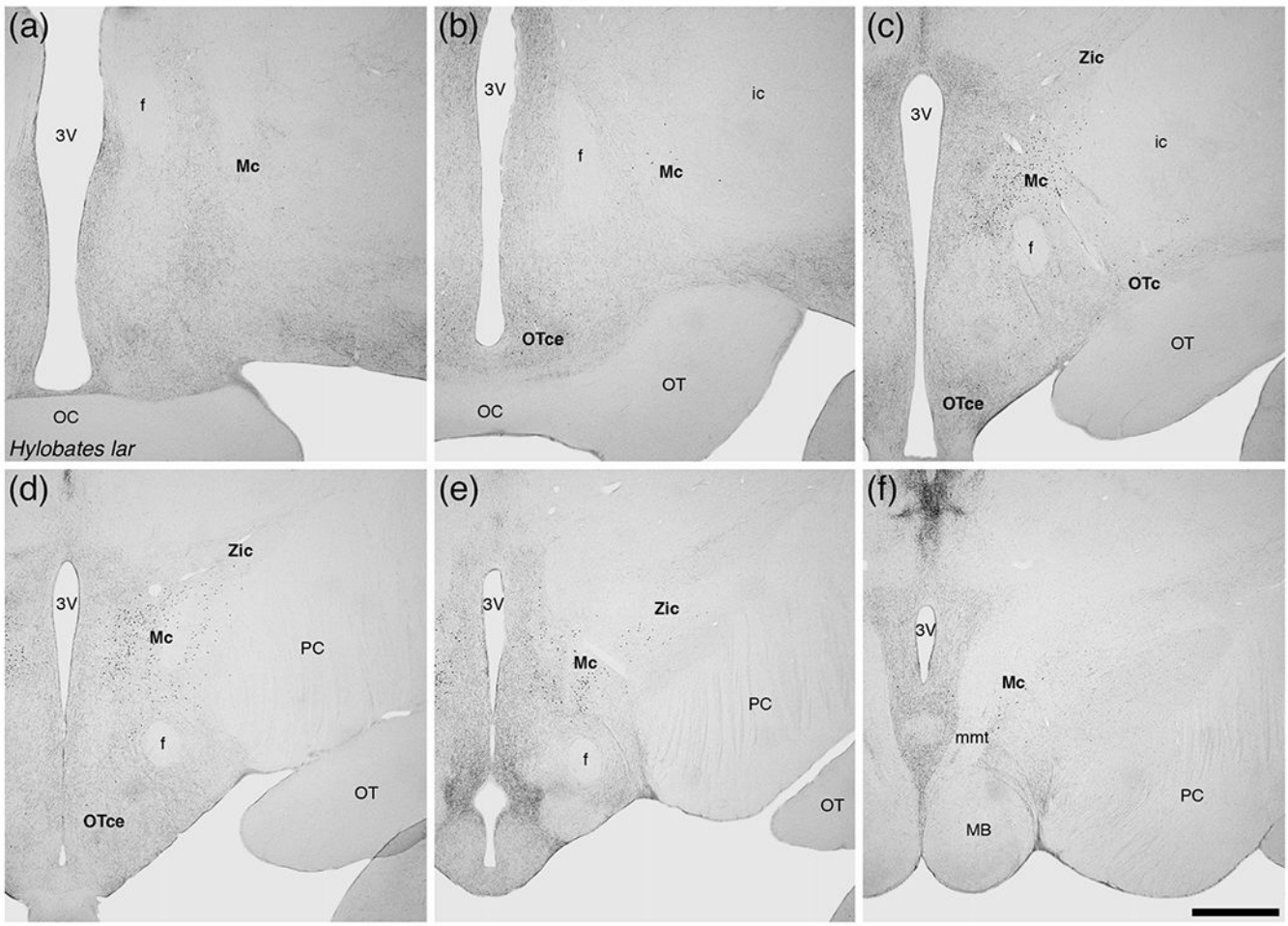

FIGURE 2.

Photomicrographs of a rostral (a) to caudal (f) series of coronal sections through the hypothalamus of the lar gibbon (*Hylobates lar*) immunostained for the orexin-A antibody. Each section is approximately 1 mm apart. Note the presence of three clusters of orexinergic neurons in the gibbon hypothalamus, the main cluster (Mc) in the perifornical region, the zona incerta cluster (Zic) which extends dorsolaterally from the Mc, and the optic tract cluster (OTc) which extends ventrolaterally from the Mc toward the optic tract (OT). In addition to these three clusters, a distinct extension of the optic tract cluster of orexinergic neurons (OTce) was observed in the anteroventral aspect of the lar gibbon hypothalamus in the tuberal region. The OTce has not been identified in other mammals to date, including other primates. In all images dorsal is to the top and the midline to the left of the image. Scale bar in (f) = 2 mm and applies to all. See list for abbreviations

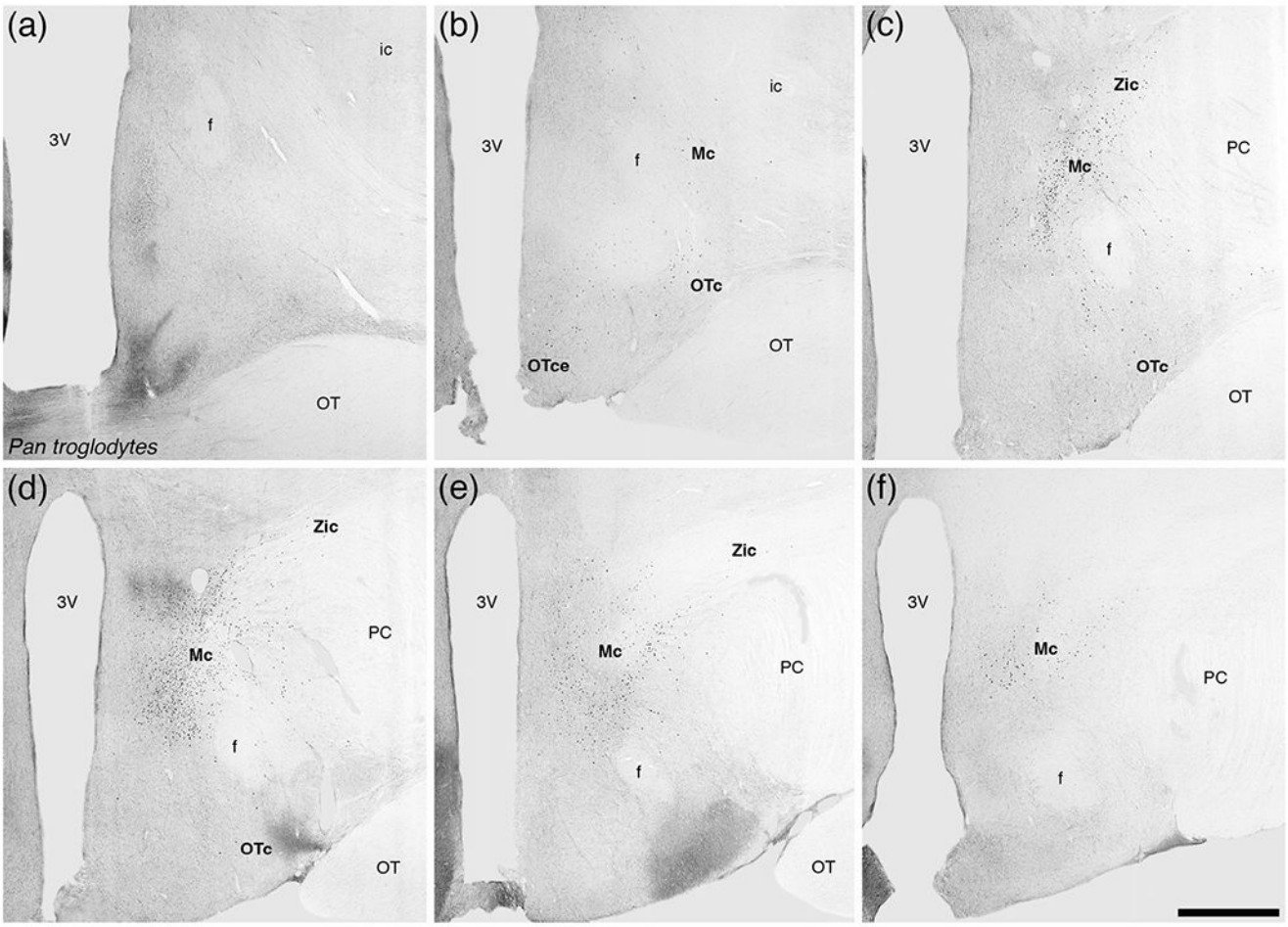

FIGURE 3.

Photomicrographs of a rostral (a) to caudal (f) series of coronal sections through the hypothalamus of the chimpanzee (*Pan troglodytes*) immunostained for the orexin-A antibody. Each section is approximately 1 mm apart. Note the presence of three clusters of orexinergic neurons in the chimpanzee hypothalamus, including the main cluster (Mc) in the perifornical region, the zona incerta cluster (Zic) which extends dorsolaterally from the Mc, and the optic tract cluster (OTc) which extends ventrolaterally from the Mc toward the optic tract (OT). In addition to these three clusters, a distinct extension of the optic tract cluster of orexinergic neurons (OTce) was observed in the anteroventral aspect of the lar gibbon hypothalamus in the tuberal region. The OTce has not been identified in other mammals to date, including other primates. In all images dorsal is to the top and the midline to the left of the image. Scale bar in (f) = 2 mm and applies to all. See list for abbreviations

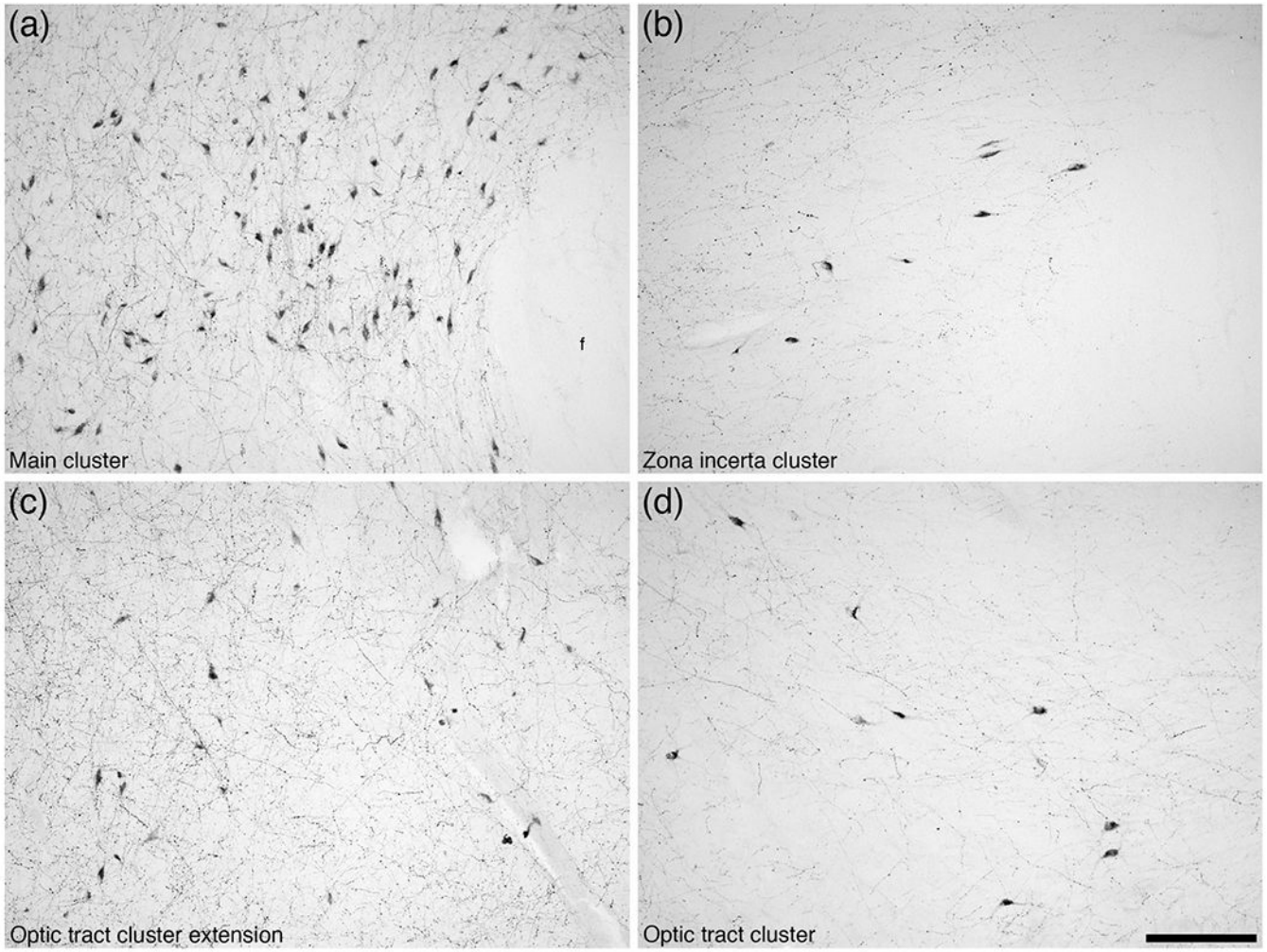

FIGURE 4.

Photomicrographs of coronal sections through the hypothalamus of the lar gibbon (*Hylobates lar*) immunostained for the orexin-A antibody showing the morphology of the orexinergic neurons. In the lar gibbon we could identify three distinct neuronal clusters, as well as a novel extension of the optic tract cluster (OTce), shown in: (a) the main cluster (Mc), located in the perifornical region that contained the majority of the orexinergic neurons; (b) the zona incerta cluster (Zic), located in the dorsolateral portion of the hypothalamus, comprised of a small number of orexinergic neurons; (c) the optic tract cluster extension (OTce), only observed to date in the apes studied herein, located in the anteroventral medial portion of the hypothalamus, comprised of a small number of orexinergic neurons; and (d) the optic tract cluster (OTc), located in the ventrolateral aspect of the hypothalamus, comprised of a small number of orexinergic neurons. In all images dorsal is to the top and medial to the left. Scale bar in (d) = 250 μm and applies to all. See list for abbreviations

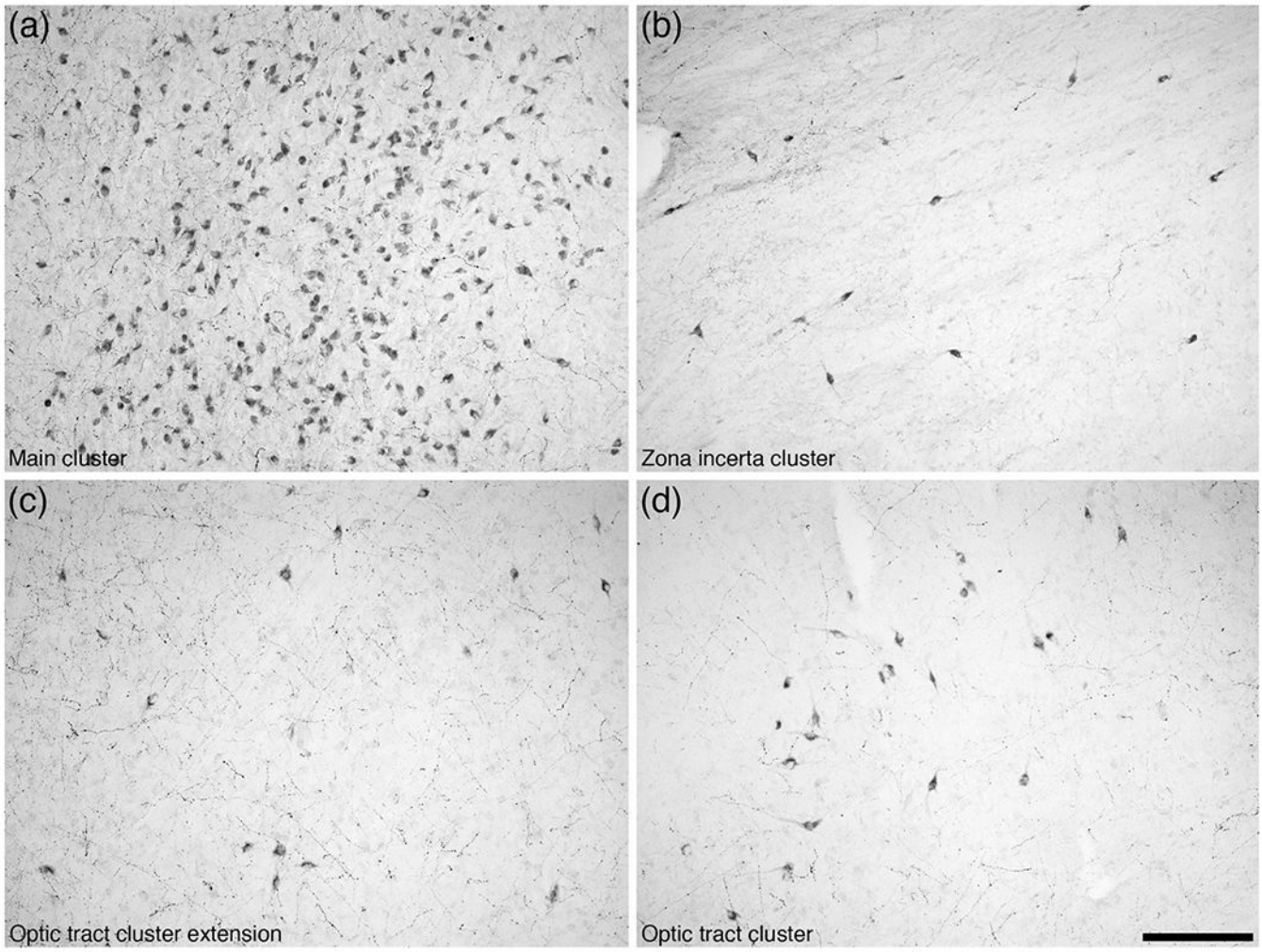

FIGURE 5.

Photomicrographs of coronal sections through the hypothalamus of the chimpanzee (*Pan troglodytes*) immunostained for the orexin-A antibody showing the morphology of the orexinergic neurons. In the chimpanzee we could identify three distinct neuronal clusters, as well as a novel extension of the optic tract cluster (OTce), shown in: (a) the main cluster (Mc), located in the perifornical region that contained the majority of the orexinergic neurons; (b) the zona incerta cluster (Zic), located in the dorsolateral portion of the hypothalamus, comprised of a small number of orexinergic neurons; (c) the optic tract cluster extension (OTce), only observed to date in the apes studied herein, located in the anteroventral medial portion of the hypothalamus, comprised of a small number of orexinergic neurons; and (d) the optic tract cluster (OTc), located in the ventrolateral aspect of the hypothalamus, comprised of a small number of orexinergic neurons. In all images dorsal is to the top and medial to the left. Scale bar in (d) = 250 μm and applies to all

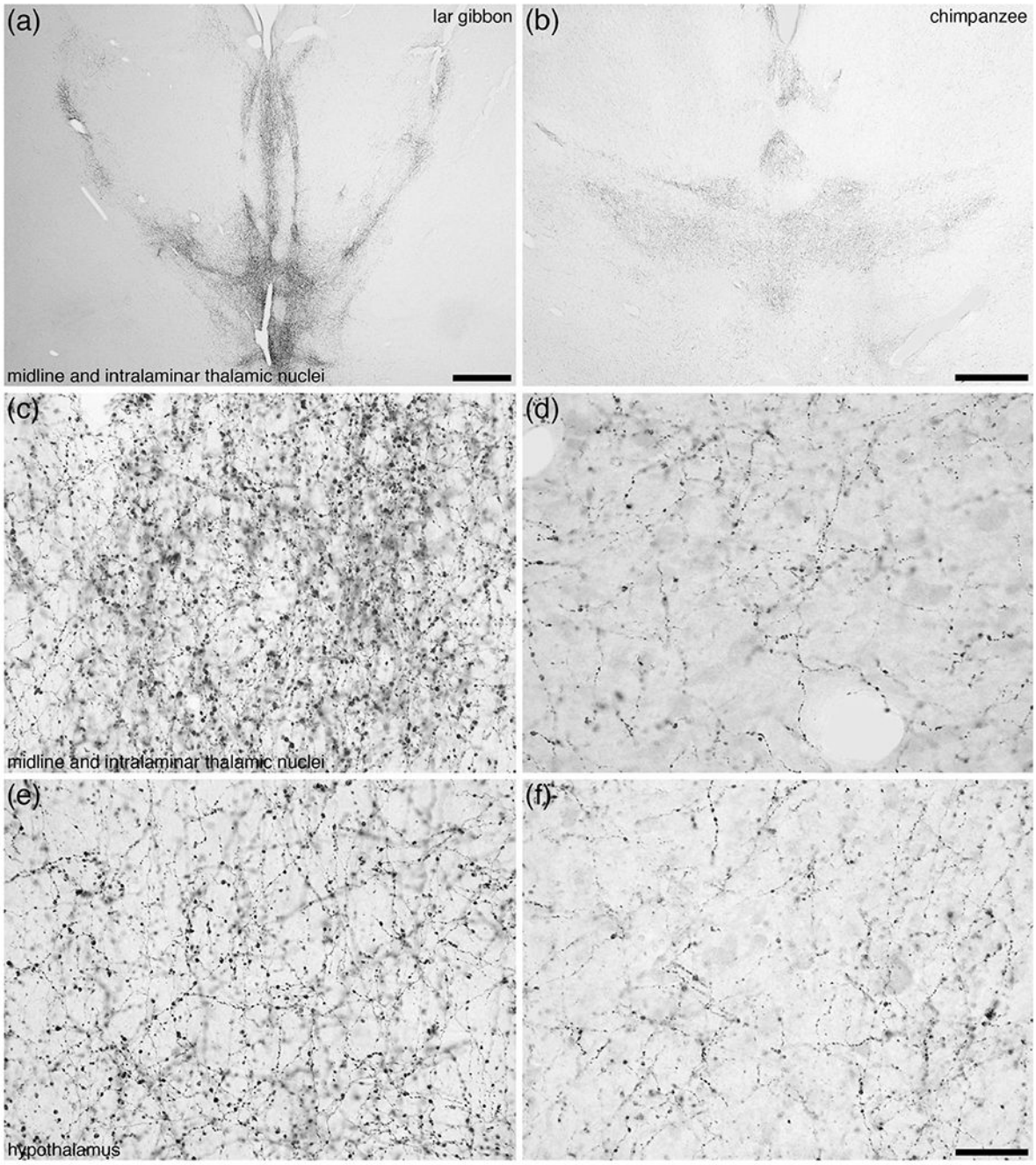

FIGURE 6.

Photomicrographs of coronal sections through the midline and intralaminar dorsal thalamic nuclei (a–d) and hypothalamus (e,f) of the lar gibbon (*Hylobates lar*, a, c, e) and chimpanzee (*Pan troglodytes*, b, d, f) immunostained for the orexin-A antibody showing the orexinergic axonal terminal networks. The low power images (a,b) in each species shows that the midline and intralaminar nuclei of the dorsal thalamus receive a dense innervation of orexinergic axons (c, d). Dense orexinergic terminal networks are also seen throughout the hypothalamus of both species (e, f). In the higher magnification images (c–f) note the

presence of both small and large boutons, with the small boutons being more numerous. In all images dorsal is to the top. Scale bars in (a) and (b) = 1 mm and apply to those images only. Scale bar in (f) = 50 μm and applies to (c) to (f)

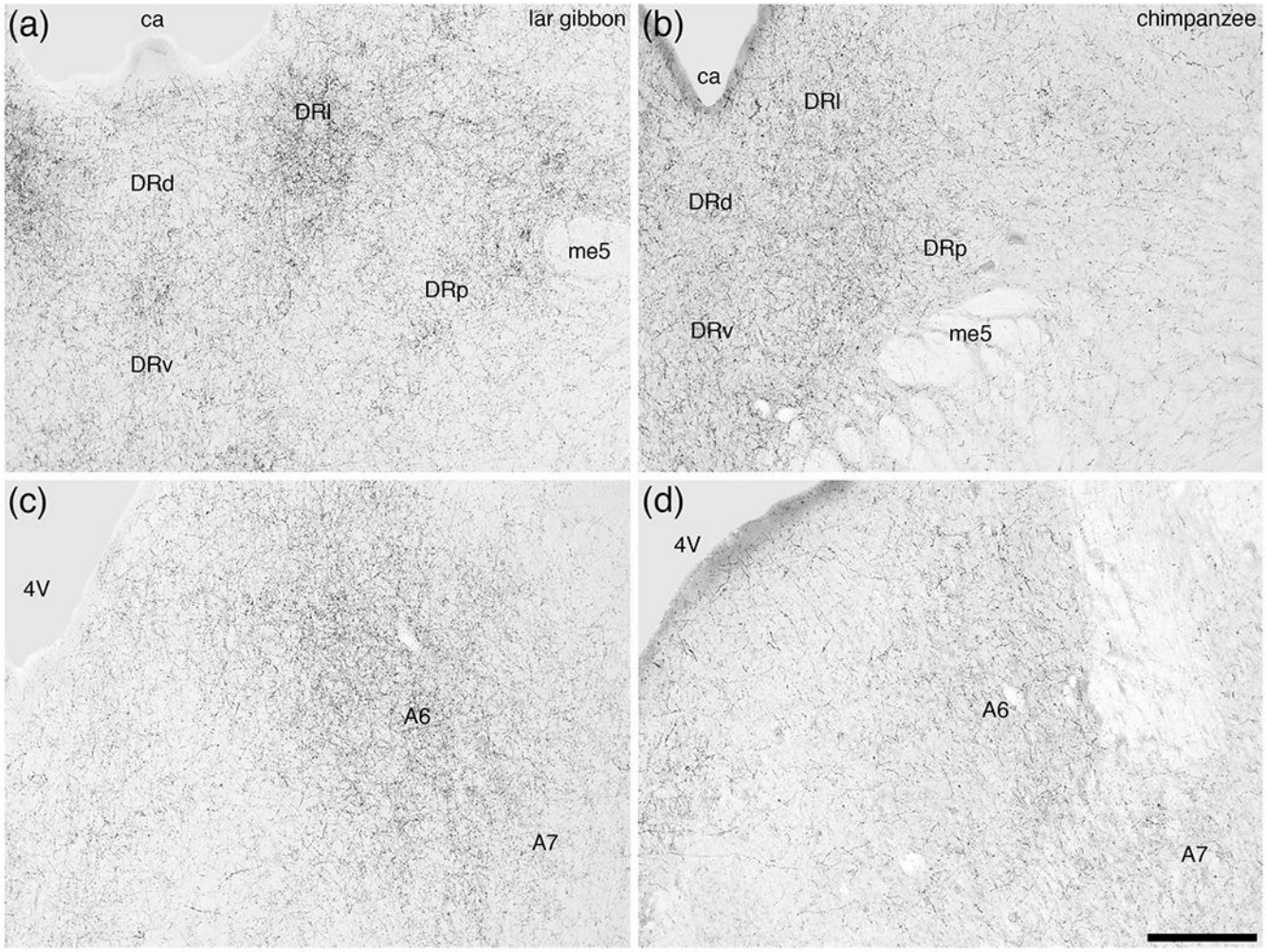

FIGURE 7.

Photomicrographs of coronal sections through the dorsal raphe nuclear cluster (a,b) and the locus coeruleus complex (c,d) of the lar gibbon (*Hylobates lar*, a, c) and chimpanzee (*Pan troglodytes*, b,d) immunostained for the orexin-A antibody showing the morphology of the orexinergic axonal terminal networks in these nuclear complexes. Note the presence of a moderate to high terminal network density in both the serotonergic dorsal raphe nuclear complex and the noradrenergic locus coeruleus complex in both species. In all images dorsal is to the top and medial to the left. Scale bar in (d) = 500 μm and applies to all images. See list for abbreviations

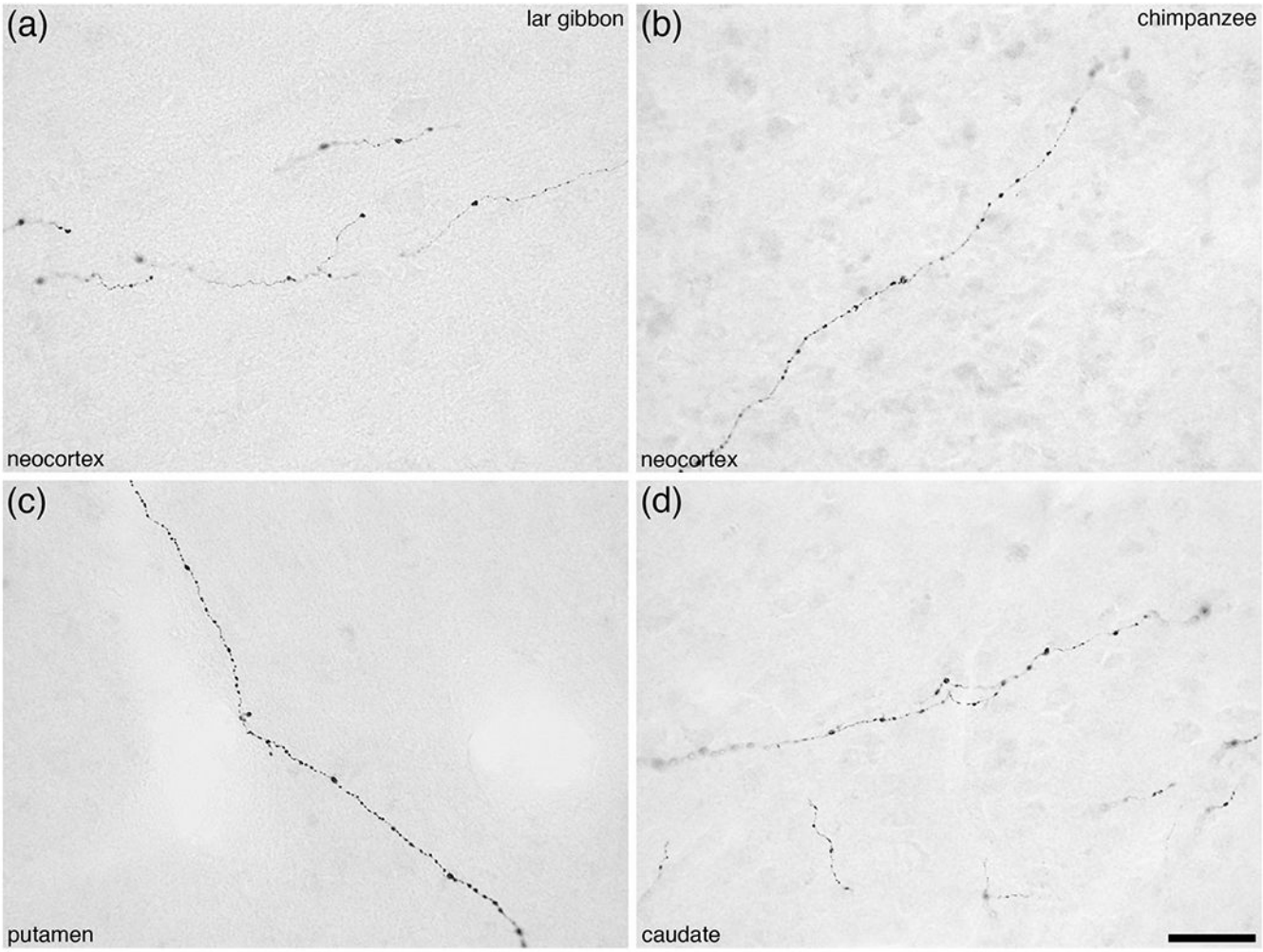

FIGURE 8.

Photomicrographs of coronal sections through the neocortex (a,b), putamen (c) and caudate nucleus (d) of the lar gibbon (*Hylobates lar*, a, c) and chimpanzee (*Pan troglodytes*, b, d) immunostained for the orexin-A antibody showing the morphology of the orexinergic axonal terminal networks. In many regions of the brain in both species low density orexinergic terminal networks were observed, and these images provide examples of what we term low density. Note also the presence of both small and large orexinergic boutons in both regions, the small boutons being more numerous. In all images dorsal is to the top and medial to the left. Scale bar in (d) = 50 μm and applies to all images

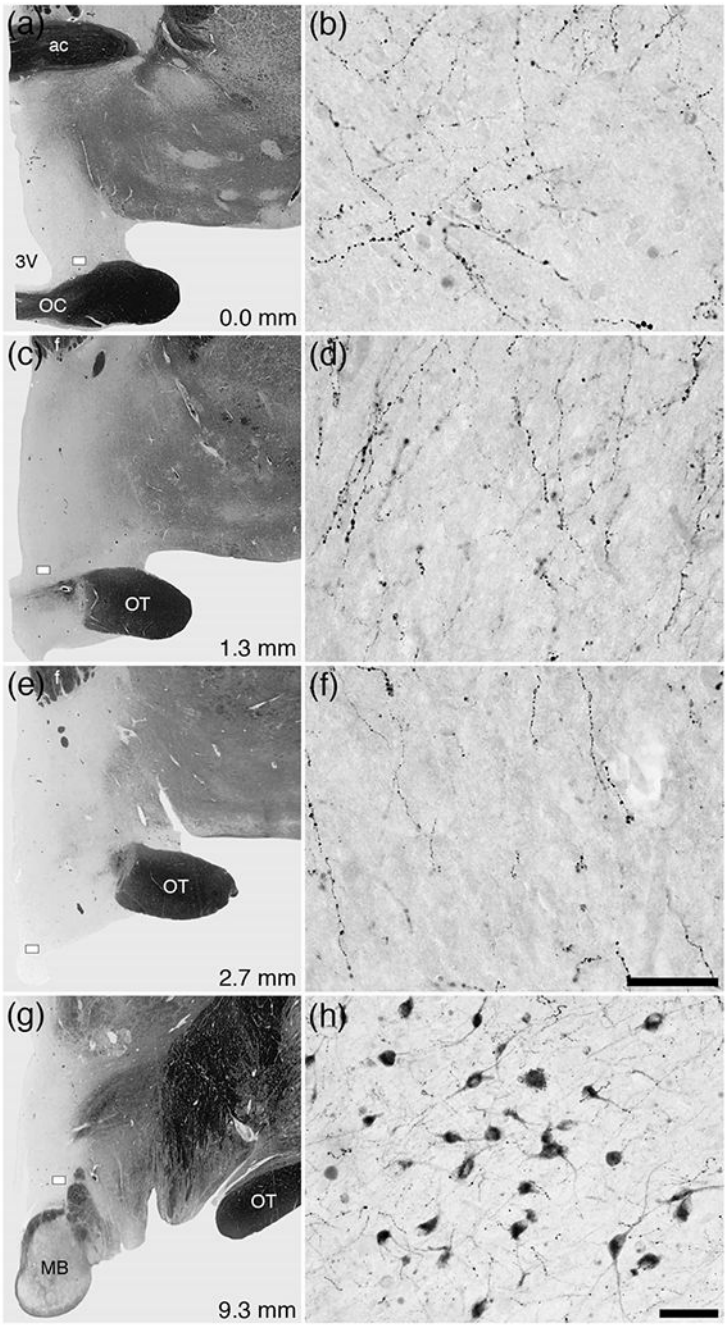

FIGURE 9.

Low magnification (a, c, e, g) and high magnification (b, d, f, h) photomicrographs of the human hypothalamus (a, c, e, g) (these images come from the reference atlas of Mai, Paxinos, & Assheuer, 2004) and immunostained for orexin (b, d, f, h) (although these images are not previously published, the sections imaged here were used in the study of Thannickal et al., 2009). The small white rectangles in a, c, e, and g represent the location where the images of the orexin stained sections in b, d, f, h were taken. Note the lack of immunostained orexinergic neurons in the tuberal region of the human hypothalamus,

despite their presence in both the lar gibbon and the chimpanzee, the clear staining of orexinergic neurons in the more caudal regions of the human hypothalamus (h), and the expression of the orexin gene in this region of the human hypothalamus (see Figures 1f and 2f of Krolewski et al., 2010). The numbers in a, c, e, g represent the distance (in millimeters) caudal to the level of the anterior commissure (ac) at which these sections were taken. Scale bar in f = 50 μm and applies to b, d and f. See list for abbreviations

TABLE 1

Stereological parameters used for estimating orexinergic neuron numbers in the hypothalamus of the lar gibbon and common chimpanzee studied

Species	Sectioning plane	Counting frame size (μm)	Sampling grid size (μm)	Disector height (μm)	Section cut thickness (μm)	Measured mounted thickness (μm)	Guard zone (μm)	Section interval	Number of sections	Number of sampling sites
Lar gibbon	Coronal	150 × 150	350 × 350	17	50	23.4	2	20	7	390
Common chimpanzee	Coronal	150 × 150	350 × 350	17	50	21.3	2	40	5	330